Mohammad Rizki Fadhil Pratama[1] / Hadi Poerwono[2] / Siswandono Siswodihardjo[2]

Molecular docking of novel 5-*O*-benzoylpinostrobin derivatives as wild type and L858R/T790M/V948R mutant EGFR inhibitor

[1] Universitas Airlangga, Doctoral Program of Pharmaceutical Science, Faculty of Pharmacy, Kampus C UNAIR Jl Dr Ir H Soekarno Mulyorejo Surabaya, East Java, Indonesia, E-mail: m.rizkifadhil@umpalangkaraya.ac.id. https://orcid.org/0000-0002-0727-4392.
[2] Universitas Airlangga, Department of Pharmaceutical Chemistry, Faculty of Pharmacy, Kampus C UNAIR Jl Dr Ir H Soekarno Mulyorejo Surabaya, East Java, Indonesia, E-mail: hadi-p@ff.unair.ac.id, prof.sis@ff.unair.ac.id. https://orcid.org/0000-0002-9241-9161, https://orcid.org/0000-0002-9579-8929.

Abstract:
Background: Previous studies have shown that 5-*O*-benzoylpinostrobin derivatives is a potential anti-breast cancer, with the highest potential being the HER2 inhibitors, is a protein's member of the epidermal growth factor receptor (EGFR) family. Overexpression of EGFR itself is known to be one of the causes of other cancer, including non-small cell lung cancer (NSCLC). Thus, it is possible that 5-*O*-benzoylpinostrobin derivatives can also inhibit the overexpression of EGFR in NSCLC. In the case of NSCLC, mutations of EGFR are often found in several amino acids, such as L858R, T790M, and V948R. This study aimed to determine the potential of 5-O-benzoylpinostrobin derivatives as an inhibitor of wild type and L858R/T790M/V948R-mutant EGFR.
Methods: Docking was performed using AutoDock Vina 1.1.2 on both wild type and L858R/T790M/V948R-mutant EGFR. Parameters observed, consisted of free energy of binding (ΔG) and amino acid interactions of each ligand.
Results: Docking results showed that all 5-*O*-benzoylpinostrobin derivatives showed a lower ΔG for both wild type and L858R/T790M/V948R-mutant EGFR, with the lowest ΔG shown by 4-methyl-5-*O*-benzoylpinostrobin and 4-trifluoromethyl-5-*O*-benzoylpinostrobin. Both the ligands have the similarity of interacting amino acids compared to reference ligands between 76.47 and 88.24%. Specifically, the ΔG of all test ligands was lower in mutant EGFR than in the wild type, which indicates the potential of the ligand as EGFR inhibitors where a mutation to EGFR occurs.
Conclusions: These results confirm that 5-*O*-benzoylpinostrobin derivatives have the potential to inhibit EGFR in both wild type and L858R/T790M/V948R-mutant.

Keywords: 5-*O*-benzoylpinostrobin, EGFR, molecular docking, NSCLC, pinostrobin
DOI: 10.1515/jbcpp-2019-0301
Received: October 13, 2019; **Accepted:** November 7, 2019

Introduction

Lung cancer is one of the leading causes of cancer-related deaths among men and women, and non-small cell lung cancer (NSCLC) comprises the majority of lung cancer [1]. Recent advances in the understanding of cell signaling pathways that control cell survival have identified genetic and regulatory aberrations that suppress cell death, promote cell division, and induce tumorogenesis [2]. One such discovery is that of the epidermal growth factor receptor (EGFR). The EGFR is a family of transmembrane receptor tyrosine kinase protein that is expressed in some normal epithelial, mesenchymal, and neurogenic tissue. Overexpression of EGFR has been reported and implicated in the pathogenesis of many human malignancies, including NSCLC [3]. The use of EGFR inhibitors in the form of monoclonal antibodies such as cetuximab, bevacizumab, nivolumab, and pembrolizumab, as well as the small-molecule kinase inhibitors (SMKIs) such as icotinib, erlotinib, and gefitinib are the first choices in the NSCLC therapy [4], [5].

In many cancer types, mutations affecting EGFR expression or activity could result in cancer or cause resistance to specific cancer therapies [6]. In the case of NSCLC, mutations of EGFR are often found in several amino acids such as L858R, T790M, and V948R [7]. Mutations in these amino acids are a problem, mainly because they can cause resistance to some EGFR inhibitors for NSCLC therapy such as erlotinib [8]. This underlies

Siswandono Siswodihardjo is the corresponding author.

the development of the new generation of SMKIs, such as osimertinib, which can adapt to mutations of some amino acids from the EGFR [9]. Therefore, the development of EGFR inhibitor compounds for NSCLC therapy needs to consider the interaction of these compounds in both wild type and mutant EGFR.

The development of EGFR inhibitors leads to the development of natural metabolite derivatives that have cytotoxic activity [10]. Some criteria of metabolites that are ideal for developing derivatives are available and can be extracted in sufficient quantities and has a pharmacophore group that can react with reagents and have been investigated and proven to have pharmacological activity [11]. One of the metabolites of natural material that is quite widely studied is pinostrobin. Pinostrobin is a flavanone present in *Boesenbergia pandurata*, which is a marker compound for these plants. The pinostrobin content is found abundant in rhizome compared to other secondary metabolites, including other well-known active metabolites such as pinocembrin and panduratin A. Pinostrobin is known to have various pharmacological activities and have been proven through laboratory tests as anticancer agent [12], [13], [14].

Pinostrobin derivatization has been done earlier, through various types of reactions. Previous research has found that the prenylation of pinostrobin can increase its cytotoxic activity against various anticancer receptors [15]. Previously, 5-*O*-benzoylpinostrobin derivatives design has been carried out by adding pinostrobin to the benzoyl with several substituent groups at the position of oxygen atom number 5. Previous *in silico* preliminary research have shown that 5-*O*-benzoylpinostrobin derivatives show potential as anti-breast cancer, as well, with the highest potential being shown as HER2 inhibitors, one of the proteins in member of the EGFR family. Thus, it is possible that 5-O-*b*enzoylpinostrobin derivatives also have potential as EGFR inhibitors, both in wild type and mutant. This study aimed to determine the potential of 5-*O*-benzoylpinostrobin derivatives as an inhibitor of wild type and L858R/T790M/V948R-mutant EGFR. The limitations of this study are the prediction tests *in silico* using the molecular docking method as a basis and guide for further *in vitro* testing.

Materials and methods

Materials

The hardware used was the ASUS A46CB series Ultrabook with an Intel™ Core i5-3337U@1.8 GHz and Windows 7 Ultimate 64-bit SP-1 operating system. The software used was HyperChem 7.5 from Hypercube Inc., OpenBabel 2.4.1 from OpenBabel.org., AutoDockTools 1.5.6 and Autodock Vina 1.1.2 software from The Scripps Research Institute Inc., PyMOL 2.3.1 from Schrodinger LLC., UCSF Chimera 1.13.1 from University of California, San Francisco, and Discovery Studio Visualizer 19.1.0.18287 from Dassault Systems BIOVIA [16], [17], [18], [19]. Information on three-dimensional structures of receptor proteins obtained from the website of Protein Data Bank (http://www.rscb.org).

Ligands preparation

The test ligands used consisted of pinostrobin and also 5-*O*-benzoylpinostrobin derivatives, as shown in Table 1. The two-dimensional structure was sketched using HyperChem 7.5. with geometry optimization *ab initio* basis set 6-31G*. Optimization was done by the Polak-Ribiere algorithm and RMS Gradient 0.1 kcal/mol. Optimization with large basis sets was carried out to obtain the ideal molecular conformation, which approves the conformation of these compounds in nature [20]. The optimized structure then changes the format from. hin to. pdb using Open Babel 2.4.1. The use of Open Babel makes it very easy to change ligands from one format to another without losing their ideal conformation [17]. Docking software used was Autodock Vina 1.1.2. The accuracy and speed of the calculation process are the main advantages of the docking process with Autodock Vina, where the disadvantages are that it requires other software to interpret the results [21]. Docking results with the most negative free energy are then stored in. pdb format using Chimera 1.13.1. Discovery Studio Visualizer 19.1.0 was used for the observation of docking results in two dimensions. The advantage of the software is that the type of amino acid interactions that occur can be observed in detail. All ligands are then given the charge and set torque by using default AutoDockTools 1.5.6 [22].

Table 1: 5-*O*-Benzoylpinostrobin derivatives test compound.

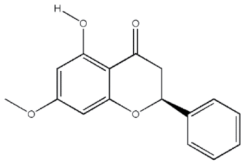

Pinostrobin

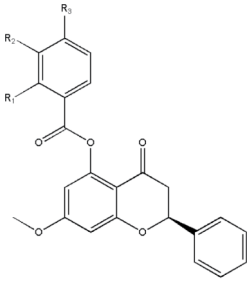

5-*O*-Benzoylpinostrobin

Compound names	Code	Functional group		
		R_1	R_2	R_3
Pinostrobin	P	–	–	–
5-*O*-Benzoylpinostrobin	BP	H	H	H
2-Chloro-5-*O*-benzoylpinostrobin	2Cl	Cl	H	H
3-Chloro-5-*O*-benzoylpinostrobin	3Cl	H	Cl	H
4-Chloro-5-*O*-benzoylpinostrobin	4Cl	H	H	Cl
2,4-Dichloro-5-*O*-benzoylpinostrobin	24Cl	Cl	H	Cl
3,4-Dichloro-5-*O*-benzoylpinostrobin	34Cl	H	Cl	Cl
4-Bromo-5-*O*-benzoylpinostrobin	4Br	H	H	Br
4-Fluoro-5-*O*-benzoylpinostrobin	4F	H	H	F
4-Nitro-5-*O*-benzoylpinostrobin	4NO	H	H	NO_2
4-Methyl-5-*O*-benzoylpinostrobin	4C	H	H	CH_3
4-Methoxy-5-*O*-benzoylpinostrobin	4OC	H	H	OCH_3
4-Trifluoromethyl-5-*O*-benzoylpinostrobin	4CF	H	H	CF
4-*t*-Butyl-5-*O*-benzoylpinostrobin	4TB	H	H	$(CH_3)_3$

Receptors preparation

The molecular structure of wild type and L858R/T790M/V948R-mutant EGFR receptor was obtained from the website of Protein Data Bank (PDB) with PDB ID 5FED and 5HG7, respectively. Both receptors are in the form of a monomer with a resolution of 2.651 Å and 1.85 Å, respectively. The receptor was downloaded in.pdb format and then the unused portion was removed, the polar hydrogen group was added and given charge. The grid box size was set as well as coordinated using AutoDockTools 1.5.6. The grid box size was obtained through the orientation process until the smallest grid box was obtained with an RMSD value below 2 Å [23]. The used chain-domain of the receptor is the active site which binds to EGFR inhibitor, in this case, ~{N}-[7-methyl-1-[(3~{R})-1-propanoylazepan-3-yl]benzimidazol-2-yl]-3-(trifluoromethyl)benzamide for 5FED and 1-{(3R,4R)-3-[({5-chloro-2-[(1-methyl-1H-pyrazol-4-yl)amino]-7H-pyrrolo[2,3-d]pyrimidin-4-yl}oxy)methyl]-4-methoxypyrrolidin-1-yl}propan-1-one for 5HG7 receptors [24], [25].

Validation of docking protocol

The docking process is preceded by a validation process with the re-docking method using reference ligands, which have been extracted from receptors as test ligands, and these reference ligands coordinate as the active site [26]. Both reference ligands from the 5FED and 5HG7 receptors were extracted and the polar hydrogen group was added, given the charge, torque and rotational bond was adjusted and then saved in the. pdbqt format. The reference ligand was then re-docked at the grid box position and size was predetermined from the orientation result [27]. The parameters observed in the validation process are root-mean-square deviation (RMSD) of reference ligand at the selected binding site using PyMOL 2.3.1. The RMSD score illustrates the average difference in ligand atom position redocking with crystallographic results, while the smaller RMSD value indicates the accuracy of the docking results that approaching the results of crystallography. The maximum value of RMSD, which is the benchmark for the docking validation process, is 2 Å, where the RMSD value less than 2 Å indicates a valid docking result [21], [28].

Molecular docking

The primary objective of the molecular docking is to identify the energetically favorable binding modes or binding pose of test ligands into the target receptor's selected binding site [29]. Docking for all test ligands were performed in the same way as the validation process with similar size and position of the grid box. The main parameter used in the docking process with Autodock Vina was the free energy of binding (ΔG) and the similarity of amino acid residues [30], [31]. The more similar amino acid residues indicate a higher probability that the test ligand will have a similar type of interaction with the reference ligand [32], [33]. As for the two-dimensional visualization of ligand-receptor, interactions were performed with Discovery Studio Visualizer v.19.1.0.18287.

Results

Validation of docking protocol

RMSD scores after redocking results from this study were provided in the range between 1.853 and 1.964 Å, which indicated that both receptors used was valid for docking purpose. Visualization of the overlay of ligand resulted from redocking with reference ligands from crystallographic results is presented in Figure 1. Overall, the redocking process shows results that can be used for the docking process. Other parameters observed in the validation process are ΔG and amino acid residues, as well as the size and coordinates of the grid box, as shown in Table 2.

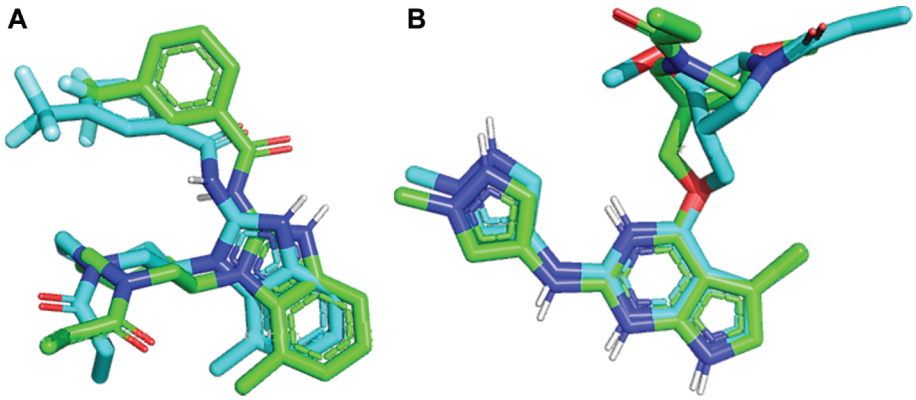

Figure 1: Overlays of redocking ligands (blue) with reference ligands from crystallography (green) at receptors (A) 5FED with RMSD 1.964 Å and (B) 5HG7 with RMSD 1.853 Å. Overlays of redocking ligands (blue) with reference ligands from crystallography (green) at receptors (A) 5FED and (B) 5HG7 visualized with PyMOL 2.3.1

Table 2: Results of the validation process.

Parameters	Value	
PDB ID	**5FED**	**5HG7**
Reference ligand	~{N}-[7-methyl-1-[(3~{R})-1-propanoylazepan-3-yl]benzimidazol-2-yl]-3-(trifluoromethyl)benzamide	1-{(3R,4R)-3-[({5-chloro-2-[(1-methyl-1H-pyrazol-4-yl)amino]-7H-pyrrolo[2,3-d]pyrimidin-4-yl}oxy)methyl]-4-methoxypyrrolidin-1-yl}propan-1-one
Grid box size (Å)	30 × 30 × 36	28 × 36 × 36
Grid box position	x: −2.124 y: 51.583 z: −20.440	x: −13.489 y: 15.359 z: −25.336
RMSD (Å)	1.964	1.853
ΔG, kcal/mol	−8.5	−8.7
Amino acid residues	718-Leu[d] 719-Gly[b] – 726-Val[d] 743-Ala[c]	718-Leu[c] 719-Gly[b] 723-Phe[b] 726-Val[c] 743-Ala[c]

745-Lys[f]	745-Lys[b]
–	775-Cys[c]
790-Thr[b]	790-Met[g]
–	791-Gln[a]
792-Leu[b]	792-Leu[b]
793-Met[a]	793-Met[a]
794-Pro[b]	794-Pro[b]
795-Phe[b]	795-Phe[b]
796-Gly[b]	796-Gly[b]
797-Cys[b]	797-Cys[c]
800-Asp[b]	–
–	841-Arg[a]
842-Asn[b]	842-Asn[b]
844-Leu[c]	844-Leu[d]
854-Thr[a]	854-Thr[b]
855-Asp[e]	–
–	856-Phe[d]

[a]Hydrogen bond; [b]Van der Waals interaction; [c]Alkyl/Pi-alkyl interaction; [d]Pi-sigma interaction; [e]Halogen; [f]Unfavorable Bump/Donor-donor; [g]Pi-Sulfur.

Molecular docking

The docking of all test ligands showed exciting results that form a consistent pattern of all test ligands: the ΔG value shown for L858R/T790M/V948R-mutant EGFR is always lower than the wild type, as presented in Table 3 and Table 4. Besides, the ΔG value of test ligands in L858R/T790M/V948R-mutant EGFR showed lower values except for pinostrobin than the reference ligands. Specifically, two test ligands have lower ΔG values than other test ligands in both wild type and L858R/T790M/V948R-mutant EGFRs consisting of 4-methyl-5-*O*-benzoylpinostrobin and 4-trifluoromethyl-5-*O*-benzoylpinostrobin. Both ligands have the same ΔG value in wild type-EGFR and only have a difference of 0.1 kcal/mol in L858R/T790M/V948R-mutant EGFR, practically showing similar potential ΔG values.

Table 3: Results of the docking of test ligands at the binding site of 5FED receptor.

Ligand	P	BP	2Cl	3Cl	4Cl	24Cl	34Cl	4Br	4F	4NO	4C	4OC	4CF	4TB
ΔG, kcal/-mol	−7.1	−8.3	−8.3	−8.6	−8.5	−8.3	−8.5	−8.2	−8.6	−8.7	−9.0	−8.3	−9.0	−8.3
Amino acid residues	–	–	–	–	–	–	–	–	–	–	–	716-Lys[b]	716-Lys[b]	–
	718-Leu[d]	718-Leu[d]	718-Leu[d]	718-Leu[d]	718-Leu[d]	718-Leu[c]	718-Leu[d]	718-Leu[d]	718-Leu[d]	718-Leu[d]	718-Leu[a]	718-Leu[d]	718-Leu[d]	718-Leu[d]
	–	–	–	–	–	719-Gly[b]	–	–	–	–	719-Gly[b]	–	719-Gly[b]	–
	–	–	–	–	–	720-Ser[b]	–	–	–	–	–	–	–	–
	–	–	–	–	–	724-Gly[b]	–	–	–	–	–	–	–	724-Gly[b]
	726-Val[c]	726-Val[c]	726-Val[b]	726-Val[c]	726-Val[c]	726-Val[c]	726-Val[c]	726-Val[d]	726-Val[b]	726-Val[c]	726-Val[c]	726-Val[b]	726-Val[c]	726-Val[d]
	728-Lys[b]	–	728-Lys[c]	728-Lys[b]	728-Lys[b]	–	728-Lys[b]	–	728-Lys[c]	728-Lys[b]	728-Lys[c]	728-Lys[c]	728-Lys[c]	–
	743-Ala[c]	743-Ala[c]	743-Ala[c]	743-Ala[c]	743-Ala[c]	743-Ala[c]	743-Ala[c]	743-Ala[c]	743-Ala[c]	743-Ala[c]	743-Ala[c]	743-Ala[c]	743-Ala[c]	743-Ala[c]
	–	745-Lys[f]	745-Lys[b]	745-Lys[c]	745-Lys[g]	745-Lys[g]	745-Lys[f]	745-Lys[f]	745-Lys[b]	745-Lys[f]	745-Lys[c]	745-Lys[f]	745-Lys[g]	745-Lys[f]
	–	–	–	–	–	–	–	762-Glu[b]	–	762-Glu[b]	–	–	–	762-Glu[b]
	–	–	–	–	–	766-Met[b]	–	–	–	–	–	–	–	–

–	–	–	–	–	–	–	775-Cys[b]	–	–	–	–	–	–
–	–	–	–	–	788-Leu[b]	–	–	–	–	–	–	–	–
790-Thr[a]	790-Thr[a]	790-Thr[a]	790-Thr[a]	790-Thr[a]	790-Thr[f]	790-Thr[a]	790-Thr[b]	790-Thr[a]	790-Thr[a]	790-Thr[a]	790-Thr[a]	790-Thr[f]	790-Thr[b]
–	–	791-Gln[b]	–	–	–	–	–	791-Gln[b]	–	–	791-Gln[b]	–	–
792-Leu[c]	792-Leu[b]	792-Leu[c]	792-Leu[c]	792-Leu[c]	792-Leu[b]	792-Leu[b]	792-Leu[b]	792-Leu[c]	792-Leu[c]	792-Leu[c]	792-Leu[c]	792-Leu[c]	792-Leu[b]
793-Met[b]	793-Met[b]	793-Met[b]	793-Met[b]	793-Met[b]	793-Met[b]	793-Met[b]	793-Met[b]	793-Met[b]	793-Met[b]	793-Met[a]	793-Met[b]	793-Met[b]	793-Met[b]
794-Pro[b]	794-Pro[b]	794-Pro[b]	794-Pro[b]	794-Pro[b]	–	794-Pro[b]	794-Pro[b]	794-Pro[b]	794-Pro[b]	794-Pro[b]	794-Pro[b]	794-Pro[e]	794-Pro[b]
795-Phe[b]	795-Phe[b]	795-Phe[b]	795-Phe[b]	795-Phe[b]	795-Phe[b]	795-Phe[b]	795-Phe[b]	795-Phe[b]	795-Phe[b]	795-Phe[b]	795-Phe[b]	795-Phe[b]	795-Phe[b]
796-Gly[b]	796-Gly[b]	796-Gly[b]	796-Gly[b]	796-Gly[b]	796-Gly[b]	796-Gly[b]	796-Gly[b]	796-Gly[b]	796-Gly[b]	796-Gly[b]	796-Gly[b]	796-Gly[a]	796-Gly[b]
797-Cys[b]	797-Cys[b]	797-Cys[b]	–	797-Cys[b]	797-Cys[c]	797-Cys[b]	797-Cys[b]	–	797-Cys[b]	–	797-Cys[b]	–	–
–	–	841-Arg[b]	–	–	–	–	–	–	–	–	841-Arg[b]	–	–
–	–	842-Asn[b]	–	–	–	–	–	842-Asn[b]	–	–	842-Asn[b]	–	–
844-Leu[c]	844-Leu[c]	844-Leu[c]	844-Leu[c]	844-Leu[c]	844-Leu[c]	844-Leu[c]	844-Leu[c]	844-Leu[c]	844-Leu[c]	844-Leu[b]	844-Leu[c]	844-Leu[b]	844-Leu[c]
–	854-Thr[b]	854-Thr[b]	854-Thr[b]	854-Thr[b]	854-Thr[b]	854-Thr[b]	854-Thr[b]	854-Thr[a]	854-Thr[b]	854-Thr[b]	854-Thr[b]	854-Thr[b]	854-Thr[b]
–	855-Asp[b]	855-Asp[b]	855-Asp[b]	855-Asp[b]	–	855-Asp[b]	855-Asp[g]	855-Asp[a]	855-Asp[b]	–	855-Asp[b]	–	855-Asp[g]

[a]Hydrogen bond; [b]Van der Waals interaction; [c]Alkyl/Pi-alkyl interaction; [d]Pi-sigma interaction; [e]Halogen; [f]Unfavorable Bump/Donor-donor; [g]Pi-Cation/Anion.

Table 4: Results of the docking of test ligands at the binding site of 5HG7 receptor.

Ligand	P	BP	2Cl	3Cl	4Cl	24Cl	34Cl	4Br	4F	4NO	4C	4OC	4CF	4TB
ΔG, kcal/-mol	−8.3	−9.4	−9.0	−9.4	−9.6	−9.2	−9.5	−9.6	−9.5	−9.5	−9.8	−9.4	−9.9	−9.6
Amino acid residues	718-Leu[d]	718-Leu[d]	718-Leu[d]	718-Leu[d]	718-Leu[d]	718-Leu[d]	718-Leu[d]	718-Leu[d]	718-Leu[d]	718-Leu[d]	718-Leu[d]	718-Leu[d]	718-Leu[d]	718-Leu[d]
	719-Gly[b]	719-Gly[b]	719-Gly[a]	719-Gly[b]	719-Gly[a]	719-Gly[a]	719-Gly[b]	719-Gly[a]	719-Gly[a]	719-Gly[a]	719-Gly[a]	719-Gly[a]	719-Gly[b]	719-Gly[b]
	720-Ser[b]	720-Ser[b]	720-Ser[b]	720-Ser[b]	–	720-Ser[b]	–	–	–	–	–	–	720-Ser[b]	720-Ser[b]
	–	–	–	–	–	–	–	–	–	–	–	–	–	721-Gly[b]
	723-Phe[b]	723-Phe[b]	723-Phe[c]	723-Phe[b]	723-Phe[b]	723-Phe[c]	723-Phe[c]	723-Phe[b]	723-Phe[b]	723-Phe[b]	723-Phe[b]	723-Phe[b]	723-Phe[b]	723-Phe[c]
	726-Val[c]	726-Val[c]	726-Val[c]	726-Val[c]	726-Val[c]	726-Val[c]	726-Val[c]	726-Val[c]	726-Val[c]	726-Val[c]	726-Val[c]	726-Val[c]	726-Val[c]	726-Val[c]
	–	728-Lys[b]	728-Lys[b]	728-Lys[b]	728-Lys[b]	728-Lys[b]	728-Lys[b]	728-Lys[b]	728-Lys[b]	728-Lys[b]	728-Lys[b]	728-Lys[b]	728-Lys[b]	–
	743-Ala[c]	743-Ala[c]	743-Ala[b]	743-Ala[c]	743-Ala[c]	743-Ala[b]	743-Ala[c]	743-Ala[c]	743-Ala[c]	743-Ala[c]	743-Ala[c]	743-Ala[c]	743-Ala[c]	743-Ala[b]
	790-Met[b]	790-Met[b]	790-Met[b]	790-Met[b]	790-Met[b]	790-Met[b]	790-Met[b]	790-Met[b]	790-Met[b]	790-Met[b]	790-Met[b]	790-Met[b]	790-Met[b]	790-Met[b]
	791-Gln[b]	–	–	–	–	–	–	–	–	–	–	–	–	–
	792-Leu[b]	792-Leu[b]	792-Leu[b]	792-Leu[b]	792-Leu[b]	792-Leu[b]	792-Leu[b]	792-Leu[b]	792-Leu[b]	792-Leu[b]	792-Leu[b]	792-Leu[b]	792-Leu[b]	792-Leu[b]

793-Met[b]	793-Met[b]	793-Met[b]	793-Met[b]	793-Met[b]	793-Met[b]	793-Met[b]	793-Met[b]	793-Met[b]	793-Met[b]	793-Met[b]	793-Met[b]	793-Met[b]	793-Met[b]
794-Pro[a]	794-Pro[b]	794-Pro[b]	794-Pro[b]	794-Pro[b]	794-Pro[b]	794-Pro[b]	794-Pro[b]	794-Pro[b]	794-Pro[b]	794-Pro[b]	794-Pro[b]	794-Pro[b]	794-Pro[b]
795-Phe[b]	795-Phe[b]	795-Phe[b]	795-Phe[b]	795-Phe[b]	795-Phe[b]	795-Phe[b]	795-Phe[b]	795-Phe[b]	795-Phe[b]	795-Phe[b]	795-Phe[b]	795-Phe[b]	795-Phe[b]
796-Gly[b]	796-Gly[b]	796-Gly[b]	796-Gly[b]	796-Gly[b]	796-Gly[b]	796-Gly[b]	796-Gly[b]	796-Gly[b]	796-Gly[b]	796-Gly[b]	796-Gly[b]	796-Gly[b]	796-Gly[b]
797-Cys[b]	797-Cys[b]	797-Cys[b]	797-Cys[b]	797-Cys[b]	797-Cys[b]	–	–	797-Cys[b]	797-Cys[b]	–	–	–	797-Cys[b]
–	841-Arg[b]	841-Arg[b]	841-Arg[a]	841-Arg[c]	841-Arg[b]	841-Arg[a]	841-Arg[c]	841-Arg[a]	841-Arg[a]	841-Arg[c]	841-Arg[a]	841-Arg[a]	841-Arg[b]
–	842-Asn[b]	842-Asn[b]	842-Asn[b]	842-Asn[b]	842-Asn[b]	842-Asn[b]	842-Asn[b]	842-Asn[b]	842-Asn[a]	842-Asn[b]	842-Asn[b]	842-Asn[a]	842-Asn[b]
844-Leu[c]	844-Leu[c]	844-Leu[c]	844-Leu[c]	844-Leu[c]	844-Leu[c]	844-Leu[c]	844-Leu[c]	844-Leu[c]	844-Leu[c]	844-Leu[c]	844-Leu[c]	844-Leu[c]	844-Leu[b]
–	854-Thr[a]	–	854-Thr[b]	854-Thr[a]	–	854-Thr[a]	854-Thr[a]	854-Thr[a]	854-Thr[a]	854-Thr[a]	854-Thr[a]	854-Thr[b]	–
856-Phe[b]	856-Phe[e]	856-Phe[e]	856-Phe[e]	856-Phe[e]	856-Phe[e]	856-Phe[e]	856-Phe[e]	856-Phe[e]	856-Phe[e]	856-Phe[e]	856-Phe[e]	856-Phe[e]	856-Phe[e]

[a]Hydrogen bond; [b]Van der Waals interaction; [c]Alkyl/Pi-alkyl interaction; [d]Pi-sigma interaction; [e]Pi-Pi stacked.

Observations of amino acid interactions show a similar trend between the results of each test ligand with the reference ligand. The similarity of test ligands except for pinostrobin against wild type-EGFR is in the range of 76.47–88.24%, while against L858R/T790M/V948R-mutant EGFR is in the range of 80–85% shown in Table 5. For observations of amino acid interaction types, the similarity is shown at a lower percentage, which is between 23.53 and 64.71% for wild type-EGFR and between 30 and 55% for L858R/T790M/V948R-mutant EGFR. Also, the two test ligands have relatively similar binding motives in both wild type and L858R/T790M/V948R-mutant EGFRs, that can be seen visually in Figure 2 and Figure 3.

Table 5: Number and percentage similarity of amino acid residues in all test ligands compared to reference ligands.

Ligands	5FED				5HG7			
	Similar amino acids		Similar amino acids interactions		Similar amino acids		Similar amino acids interactions	
	Σ	%	Σ	%	Σ	%	Σ	%
P	11	64.71	7	41.18	15	75	7	35
BP	14	82.35	9	52.94	17	85	9	45
2Cl	15	88.24	8	47.06	16	80	6	30
3Cl	14	82.35	7	41.18	17	85	11	55
4Cl	14	82.35	8	47.06	17	85	8	40
24Cl	13	76.47	6	35.29	16	80	6	30
34Cl	14	82.35	9	52.94	16	80	9	45
4Br	14	82.35	11	64.71	16	80	8	40
4F	14	82.35	8	47.06	17	85	9	45
4NO	14	82.35	8	47.06	17	85	8	40
4C	13	76.47	6	35.29	16	80	8	40
4OC	15	88.24	9	52.94	16	80	9	45
4CF	13	76.47	10	58.82	16	80	10	50
4TB	13	76.47	4	23.53	16	80	7	35

Note: percentages were compared to the amount and type of amino acid residue interactions of reference ligands.

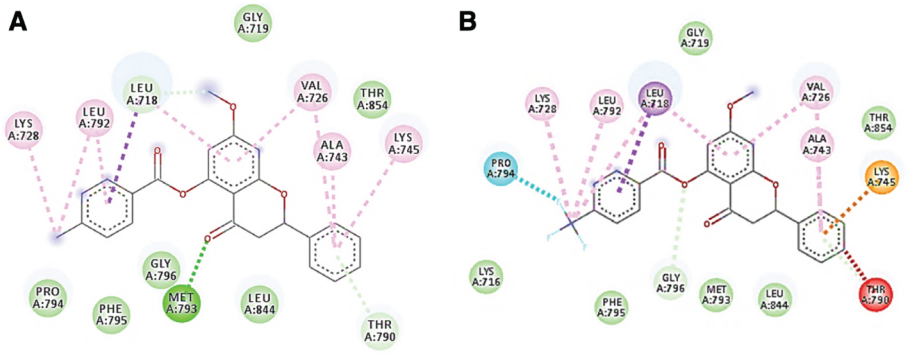

Figure 2: Interactions of (A) 4-methyl-5-*O*-benzoylpinostrobin and (B) 4-trifluoromethyl-5-*O*-benzoylpinostrobin in amino acid residues from 5FED receptors. Interactions of (A) 4-methyl-5-O-benzoylpinostrobin and (B) 4-trifluoromethyl-5-O-benzoylpinostrobin in amino acid residues from 5FED receptors visualized with Discovery Studio Visualizer v.19.1.0.18287.

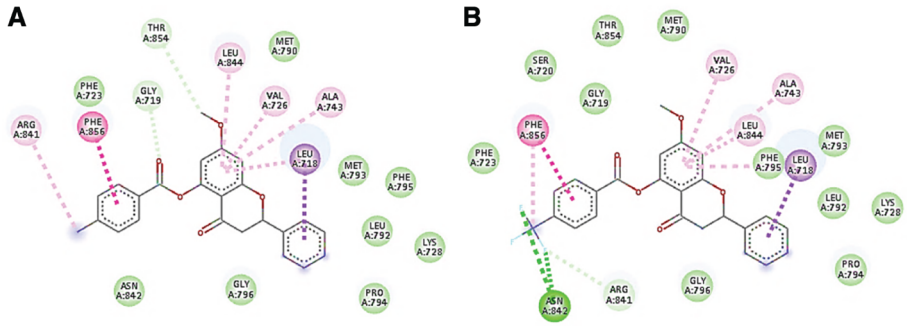

Figure 3: Interactions of (A) 4-methyl-5-*O*-benzoylpinostrobin and (B) 4-trifluoromethyl-5-*O*-benzoylpinostrobin in amino acid residues from 5HG7 receptors. Interactions of (A) 4-methyl-5-O-benzoylpinostrobin and (B) 4-trifluoromethyl-5-O-benzoylpinostrobin in amino acid residues from 5HG7 receptors visualized with Discovery Studio Visualizer v.19.1.0.18287.

Discussion

The docking protocol is done by using energy range 3, exhaustiveness 18, and the number of modes 9. In addition to exhaustiveness, values for other parameters were the default values of Autodock Vina. The value of exhaustiveness is increased from 8 to 18, to increase the robustness of the docking performed [30]. Validation is carried out at the active site of both receptors using reference ligands to determine the size and coordinates of each grid box. Molecular docking was performed using configuration settings similar to the validation process, with changes to the test ligand file used [34]. However, one consideration in determining the size of the grid box is the size of the test ligands, so that the size of the test ligand does not exceed the specified grid box size [35]. The RMSD value of the validation results is relatively high, which is in the range of 1.8–1.9 Å, although it still meets the requirements under 2 Å. The reliability of docking results is determined by the value of RMSD, where the higher RMSD value indicates a higher probability that the position of crystallography ligand will be different from the docking ligand position [36].

One interesting finding from this research is that all the test ligands have lower ΔG values in L858R/T790M/V948R-mutant than wild type-EGFR. The lower ΔG value in the L858R/T790M/V948R-mutant compared to the wild type-EGFR indicates the potential of the test ligand to anticipate the occurrence of NSCLC resistance to anticancer compounds [37], where mutations in the three amino acids L858R, T790M, and V948R are the main causes of resistance in NSCLC [38]. In other words, all test ligands are predicted to be able to adapt to mutations from EGFR and still maintain their potential as inhibitors despite mutations in some amino acids. A similar trait is shared by third-generation EGFR inhibitors that have been marketed, such as osimertinib or TAS-121, a novel EGFR inhibitor which is still under investigation [39], [40]. However, both can overcome different types of mutations, although basically, they are focused on mutations in the T790M.

Among all test ligands, the lowest ΔG value in both types of EGFR receptors was shown by 4-trifluoromethyl-5-*O*-benzoylpinostrobin and 4-methyl-5-*O*-benzoylpinostrobin. Observations of the Hansch QSAR parameters of the two compounds showed quite different results from the parent compounds,

but were not interconnected [41]. When compared with 5-O-benzoylpinostrobin, 4-trifluoromethyl-5-*O*-benzoylpinostrobin has higher hydrophobicity (π) and electronic (σ) parameters. The values of the two parameters are relatively not much different compared to 4-bromo-5-*O*-benzoylpinostrobin. Therefore, the ΔG value of 4-bromo-5-*O*-benzoylpinostrobin in L858R/T790M/V948R-mutant EGFR is also not too different from that shown by 4-trifluoromethyl-5-*O*-benzoylpinostrobin (0.3 kcal/mol). While for 4-methyl-5-*O*-benzoylpinostrobin, the π parameter is relatively lower than 4-trifluoromethyl-5-*O*-benzoylpinostrobin, but is still higher than 5-*O*-benzoylpinostrobin, while the σ parameter is lower than 5-*O*-benzoylpinostrobin. In other words, when 4-trifluoromethyl-5-*O*-benzoylpinostrobin tends to be hydrophobic and polar, 4-methyl-5-*O*-benzoylpinostrobin is relatively more non-polar. However, highly hydrophobic test ligands such as 4-*t*-butyl-5-*O*-benzoylpinostrobin and very polar ones like 4-nitro-5-*O*-benzoylpinostrobin show ΔG values not as low as both. This research shows that other parameters affect the value of ΔG besides the two parameters.

Prediction of similarity of amino acids that interact and the type of interaction are important parameters to be evaluated from docking results. There is a possibility that higher the amino acid similarity that interacts and the type of interaction, the higher is the chance that the test ligand will have similar activity with reference ligands [42]. Observation in the similarity of the amino acid that interacts with the test ligand as well as the type of interaction that occurs from each ligand show results that vary with the ΔG value of each test ligand without conclusions. Although the types of amino acids that interact, are in a relatively high range of similarity, the types of interactions that occur tend to be more different. The different types of interactions are caused by differences in the pharmacophores of each ligand, where different types of pharmacophores will cause different types of interactions [43]. Thus, an analysis of each type of amino acid that interacts with all test ligands was carried out.

Overall, amino acids that interact with both the test ligand and reference ligands are 718-Leu, 726-Val, 743-Ala, 790-Thr, 792-Leu, 793-Met, 795-Phe, 796-Gly, and 844-Leu for wild type-EGFR, and 718-Leu, 719-Gly, 723-Phe, 726-Val, 743-Ala, 790-Met, 792-Leu, 793-Met, 794-Pro, 795-Phe, 796-Gly, 844 -Leu, and 856-Phe for L858R/T790M/V948R-mutant EGFR. From the results of this study it can be seen that there are more amino acids in L858R/T790M/V948R-mutant compared to wild type EGFR (13 vs. 9). Hence, it was observed that all amino acids in wild type also interact with L858R/T790M/V948R-mutant EGFR. However, four amino acids interact with the L858R/T790M/V948R-mutant but not with the wild type-EGFR of all test ligands, consisting of 719-Gly, 723-Phe, 795-Phe, and 856-Phe.

This research also shows interesting results where all test ligands interact with amino acids at position 790, both in the form of wild type (threonine) and mutated (methionine). In the wild type-EGFR, the interaction at position 790 is influenced by the phenyl group, which means that the role of the interaction at that position is an "anchor." The variation of the substituents of the benzoyl group does not directly influence the interaction of the amino acid. While in L858R/T790M/V948R-mutant EGFR, the interaction of amino acids is shown by the 7-methoxy group, which also has no direct effect on variations in the substituents of the benzoyl group. One factor that plays a role in the differences in position of the test ligand is the difference in tertiary structure of the two types of EGFR [44]. Mutations in one amino acid located at a particular position can dramatically affect the tertiary or quaternary structure of a receptor protein so that it can affect its biological function [45]. In other words, 5-*O*-benzoylpinostrobin derivatives have different interaction approaches for the wild type and L858R/T790M/V948R-mutant EGFR.

Conclusions

In conclusion, this study has successfully demonstrated the potential of 5-*O*-benzoylpinostrobin derivatives as inhibitors of both wild type and L858R/T790M/V948R-mutant EGFR. In general, all test ligands have a lower ΔG value against L858R/T790M/V948R-mutant than the wild type-EGFR, showing their potential as an inhibitor of mutated EGFR occurring in NSCLC. The enormous potential is shown by two ligands consisting of 4-methyl-5-*O*-benzoylpinostrobin and 4-trifluoromethyl-5-*O*-benzoylpinostrobin, where both show the lowest ΔG value in both wild type and L858R/T790M/V948R-mutant EGFRs. The indicated ΔG value is even lower than the reference ligands in both receptors, with a fairly high percentage of amino acid interaction similarities with the reference ligands in the range of 76.47–88.24%. However, the limitation of this study is that the study is only limited to the *in silico* prediction stage. Further, *in vitro* testing with a cytotoxic assay must be carried out to re-evaluate the potential of 5-*O*-benzoylpinostrobin derivatives as both wild type and L858R/T790M/V948R-mutant EGFRs inhibitors.

Acknowledgments

This paper has been presented at the 8th APPEN Conference and 2nd HPC Conference on 8–9th October 2019, Universitas Airlangga, Surabaya, Indonesia.

Research funding: None declared.

Author contributions: All authors have contributed equally to the preparation of this manuscript. MRFP plays a role in the validation and docking process. HP and S play an equal role in the design of test compounds as well as research designs.

Competing interests: All authors declare that there is no conflict of interest regarding the publication of this article.

References

[1] De Groot PM, Wu CC, Carter BW, Munden RF. The epidemiology of lung cancer. Transl Lung Cancer Res 2018;7:220–33.
[2] Levine B, Kroemer G. Biological Functions of autophagy genes: a disease perspective. Cell 2019;176:11–42.
[3] Bethune G, Bethune D, Ridgway N, Xu Z. Epidermal growth factor receptor (EGFR) in lung cancer: an overview and update. J Thorac Dis 2010;2:48–51.
[4] Silva AP, Coelho PV, Anazetti M, Simioni PU. Targeted therapies for the treatment of non-small-cell lung cancer: monoclonal antibodies and biological inhibitors. Hum Vaccin Immunother 2017;13:843–53.
[5] Ni J, Zhang L. Evaluation of three small molecular drugs for targeted therapy to treat nonsmall cell lung cancer. Chin Med J 2016;129:332–40.
[6] Sigismund S, Avanzato D, Lanzetti L. Emerging functions of the EGFR in cancer. Mol Oncol 2018;12:3–20.
[7] Kannan S, Venkatachalam G, Lim HH, Surana U, Verma C. Conformational landscape of the epidermal growth factor receptor kinase reveals a mutant specific allosteric pocket. Chem Sci 2018;9:5212–22.
[8] Tang J, Salama R, Gadgeel SM, Sarkar FH, Ahmad A. Erlotinib resistance in lung cancer: current progress and future perspectives. Front Pharmacol 2013;4:15.
[9] Le T, Gerber DE. Newer-generation egfr inhibitors in lung cancer: how are they best used? Cancer 2019;11:E366.
[10] Sangpheak K, Tabtimmai L, Seetaha S, Rungnim C, Chavasiri W, Wolschann P, et al. Biological evaluation and molecular dynamics simulation of chalcone derivatives as epidermal growth factor-tyrosine kinase inhibitors. Molecules 2019;24:1092.
[11] Atanasov AG, Waltenberger B, Pferschy-Wenzig EM, Linder T, Wawrosch C, Uhrin P, et al. Discovery and resupply of pharmacologically active plant-derived natural products: A review. Biotechnol Adv 2015;33:1582–614.
[12] Jaudan A, Sharma S, Malek SN, Dixit A. Induction of apoptosis by pinostrobin in human cervical cancer cells: Possible mechanism of action. PLoS One 2018;13:e0191523.
[13] Tan BC, Tan SK, Wong SM, Ata N, Rahman NA, Khalid N. Distribution of flavonoids and cyclohexenyl chalcone derivatives in conventional propagated and in vitro-derived field-grown Boesenbergia rotunda (L.) Mansf. Evid Based Complement Alternat Med 2015;2015:451870.
[14] Junior WA, Gomes DB, Zanchet B, Schonell AP, Diel KA, Banzato TP, et al. Antiproliferative effects of pinostrobin and 5,6-dehydrokavain isolated from leaves of Alpinia zerumbet. Rev Bras Farmacogn 2017;27:592–8.
[15] Poerwono H, Sasaki S, Hattori Y, Higashiyama K. Efficient microwave-assisted prenylation of pinostrobin and biological evaluation of its derivatives as antitumor agents. Bioorg Med Chem Lett 2010;20:2086–9.
[16] Trott O, Olson AJ. AutoDock Vina: improving the speed and accuracy of docking with a new scoring function, efficient optimization and multithreading. J Comput Chem 2010;31:455–61.
[17] O'Boyle NM, Banck M, James CA, Vandermeersch T, Hutchison GR. Open Babel: an open chemical toolbox. J Cheminformatics 2011;3:33.
[18] Yuan S, Chan S, Hu Z. Using PyMOL as a platform for computational drug design. Wiley Interdiscip Rev Comput Mol Sci 2017;7:e1298.
[19] Pettersen EF, Goddard TD, Huang CC, Couch GS, Greenblatt DM, Meng EC, et al. UCSF Chimera–a visualization system for exploratory research and analysis. J Comput Chem 2004;25:1605–12.
[20] Pratama MR, Sutomo S. Chemical structure optimization of lupeol as ER-A and HER2 inhibitor. Asian J Pharm Clin Res 2018;11:298–303.
[21] Pagadala NS, Syed K, Tuszynski J. Software for molecular docking: a review. Biophys Rev 2017;9:91–102.
[22] Forli S. Charting a path to success in virtual screening. Molecules 2015;20:18732–58.
[23] Feinstein WP, Brylinski M. Calculating an optimal box size for ligand docking and virtual screening against experimental and predicted binding pockets. J Cheminform 2015;7:18.
[24] Lelais G, Epple R, Marsije TH, Long YO, McNeill M, Chen B, et al. Discovery of (R,E)-N-(7-Chloro-1-(1-[4-(dimethylamino)but-2-enoyl]azepan-3-yl)-1H-benzo[d]imidazol-2-yl)-2-methylisonicotinamide (EGF816), a novel, potent, and WT sparing covalent inhibitor of oncogenic (L858R, ex19del) and Resistant (T790M) EGFR mutants for the treatment of EGFR mutant non-small-cell lung cancers. J Med Chem 2016;59:6671–89.
[25] Cheng H, Nair SK, Murray BW, Almaden C, Bailey S, Baxi S, et al. Discovery of 1-{(3R,4R)-3-[({5-Chloro-2-[(1-methyl-1H-pyrazol-4-yl)amino]-7H-pyrrolo[2,3-d]pyrimidin-4-yl}oxy)methyl]-4-methoxypyrrolidin-1-yl}prop-2-en-1-one (PF-06459988), a potent, WT Sparing, irreversible inhibitor of T790M-containing EGFR mutants. J Med Chem 2016;59:2005–24.
[26] Srivastava JK, Pillai GG, Bhat HR, Verma A, Singh UP. Design and discovery of novel monastrol-1,3,5-triazines as potent anti-breast cancer agent via attenuating epidermal growth factor receptor tyrosine kinase. Sci Rep 2017;7:5851.

[27] Megantara S, Iwo MI, Levita J, Ibrahim S. Determination of ligand position in aspartic proteases by correlating Tanimoto coefficient and binding affinity with root mean square deviation. J App Pharm Sci 2016;6:125–9.
[28] Castro-Alvarez A, Costa AM, Vilarrasa J. The performance of several docking programs at reproducing protein-macrolide-like crystal structures. Molecules 2017;22:E136.
[29] Atkovska K, Samsonov SA, Paszkowski-Rogacz M, Pisabarro MT. Multipose binding in molecular docking. Int J Mol Sci 2014;15:2622–45.
[30] Forli S, Huey R, Pique ME, Sanner M, Goodsell DS, Olson AJ. Computational protein-ligand docking and virtual drug screening with the AutoDock suite. Nat Protoc 2016;11:905–19.
[31] Natesan S, Subramaniam R, Bergeron C, Balaz S. Binding affinity prediction for ligands and receptors forming tautomers and ionization species: inhibition of mitogen-activated protein kinase-activated protein kinase 2 (MK2). J Med Chem 2012;55:2035–47.
[32] Pratama MR, Suratno S, Mulyani E. Antibacterial activity of akar kuning (Arcangelisia flava) secondary metabolites: molecular docking approach. Asian J Pharm Clin Res 2018;11:447–51.
[33] Singh H, Srivastava HK, Raghava GP. A web server for analysis, comparison and prediction of protein ligand binding sites. Biol Direct 2016;11:14.
[34] Miller RL, Thompson AA, Trapella C, Guerrini R, Malfacini D, Patel N, et al. The importance of ligand-receptor conformational pairs in stabilization: spotlight on the N/OFQ G protein-coupled receptor. Structure 2015;23:2291–9.
[35] Ferreira LG, dos Santos RN, Oliva G, Andricopulo AD. Molecular docking and structure-based drug design strategies. Molecules Molecules Molecules Molecules 2015;20:13384–421.
[36] Ramirez D, Caballero J. Is it reliable to take the molecular docking top scoring position as the best solution without considering available structural data? Molecules 2018;23:1038.
[37] Le T, Gerber DE. Newer-Generation EGFR Inhibitors in lung cancer: how are they best used? Cancers 2019;11:366.
[38] Yun CH, Mengwasser KE, Toms AV, Woo MS, Greulich H, Wong KK, et al. The T790M mutation in EGFR kinase causes drug resistance by increasing the affinity for ATP. Proc Natl Acad Sci U S A 2008;105:2070–5.
[39] Minari R, Bordi P, Tiseo M. Third-generation epidermal growth factor receptor-tyrosine kinase inhibitors in T790M-positive non-small cell lung cancer: review on emerged mechanisms of resistance. Transl Lung Cancer Res 2016;5:695–708.
[40] Nishio M, Murakami H, Ohe Y, Hida T, Sakai H, Kasahara K, et al. Phase I study of TAS-121, a third-generation epidermal growth factor receptor (EGFR) tyrosine kinase inhibitor, in patients with non-small-cell lung cancer harboring EGFR mutations. Invest New Drugs 2019;(37):1207–17.
[41] Kubinyi H. QSAR: Hansch Analysis and Related Approaches. In: Mannhold R, Krogsgaard-Larsen P, Timmerman H, editors. QSAR: hansch analysis and related approaches. Weinheim: VCH Verlagsgesellschaft mbH, 1993:21–6.
[42] Pratama MR, Gusdinar T. Docking study of secondary metabolites from Glycyrrhiza glabra as PPAR-γ agonist. Biointerface Res Appl Chem 2019;9:4006–10.
[43] Mortier J, Dhakal P, Volkamer A. Truly Target-focused pharmacophore modeling: a novel tool for mapping intermolecular surfaces. Molecules 2018;23:1959.
[44] Martin-Fernandez ML, Clarke DT, Roberts SK, Zanetti-Domingues LC, Gervasio FL. Structure and dynamics of the EGF receptor as revealed by experiments and simulations and its relevance to non-small cell lung cancer. Cells 2019;8:316.
[45] Schaefer C, Rost B. Predict impact of single amino acid change upon protein structure. BMC Genomics 2012;13:S4.

Supplementary Material: The online version of this article offers supplementary material (DOI: https://doi.org/10.1515/jbcpp-2019-0301).